Extraction of Coronary Arteries by Using a Sequence of X-Ray Angiographic Images

Chih-Yang Lin [a] , Yu-Tai Ching [a] , SY James Chen [b]

[a] Department of Computer and Information Science, National Chiao Tung Univerity, Hsin Chu, Taiwan

[b] Division of Cardiology Department of Medicine, University of Colorado, Stenver, Colorado, USA.

ABSTRACT

A method was developed for extraction coronary arteries from a contiguous sequence of angiographic images. Since coronary artery in the image usually has poor local contrast and has ribs, spine, and other tissues in the background. We remove the background using the information of temporal continuity. A set of multi-size matched filters process to enhance vessels from poor local contrast. The wavelet transformation based method is then employed to remove noise to enhance the image quality. We also design a stencil mask to remove the stationary tissues further.

Keywords: Artery, Angiogram, Segmentation, Extraction

1. INTRODUCTION

Accurate analysis of coronary arteries in digital angiographic images is valuable and important to clinical needs. Generally, coronary angiograms are still the most common modality for physicians to accurately assess the severity of coronary arterial stenosis. Extraction of a coronary arterial segment or entire tree from 2-D angiograms is regarded as a crucial process to facilitate quantitative coronary analysis.

The major difficulty with the extraction of angiogram is that angiographic images usually have poor local contrast. And the ribs, spine, and other tissues are also shown in the image. Traditional edge detection algorithms [1]-[6] cannot effectively detect the edges. Furthermore, we generally need to extract the blood vessel as whole. Previous methods to extract vessels include model-base [8]-[10], tracking-base [11]-[13], classifier-base [14], and filter-base [15]-[17]. A matched filter [15] used a Gaussian vessel model filter set for detecting blood vessels in optical images of the retina. In [14], the matched filter was extended to two-dimension space. The extension is based on the observation that a vessel has a fixed direction for a short length. Since vessels may appear in any orientation, the filters were implemented using twelve 16 pixels by 16 pixels masks for different directions. The filter was design to detect vessel with fixed diameters. The fixed diameter assumption is fine to segment the retina since retina has almost the same vessel size. It is more difficult to extract the coronary arties than to extract the retina since the vessel diameters of coronary arteries are different. The diameter of primary artery is generally larger than the secondary artery. In this work, we present a method to segment the coronary arteries from a sequence of angiographics images. The proposed method consists of steps of background removal, vessel enhancement, and finally the vessel identification. In the next section, we present the method. The experimental results are shown in Section 3.

2. METHODS

The proposed methods consist of five steps. In the first step, we apply Fourier analysis in temporal to eliminate the stationary background for a sequence of angiographic images. In the second step, a set of multiple sized matched filters is applied to enhance the coronary arteries. The third step employs a wavelet transformation based method in spatial domain to remove noise so that the coronary arteries are further enhanced. The fourth step is the cluster analysis. This step is designed to remove that were difficult to remove in step 1. Since the vessels are a connected component in an angiographic image. We use the property to design a stencil mask to remove the smaller connected components. Finally, we apply certain threshold value that depends on the histogram to obtain the segmented arteries.

Given a sequence of angiographic images, their Fourier transformation [18] consists of a single peak at a frequency of 0 (a single DC term), which the stationary tissues take place in. The stationary and slow motion parts are normally ribs, spine and other tissues, which appear in the image as background. Thus we apply Fourier transformation in temporal to remove those stationary components.

For a sequence of T images, denote as $f(x, y, t)$, the discrete Fourier transformation pair are

Medical Imaging 2001: Image Processing, Milan Sonka, Kenneth M. Hanson, Editors,
Proceedings of SPIE Vol. 4322 (2001) © 2001 SPIE · 1605-7422/01/$15.00

$$F(x,y,k)=\sum_{t=0}^{T-1} f(x,y,t)e^{-j2\pi kt/T} \quad 0\le k\le T-1, \tag{1}$$

and

$$f(x,y,t)=\sum_{k=0}^{T-1} F(x,y,k)e^{j2\pi kt/T} \quad 0\le t\le T-1. \tag{2}$$

We apply Eq. (1) for a sequence of angiograms. Since DC term and low frequency are the stationary background, we multiply Eq. (1) by $H(x,y,k)$ as shown in Eq. (3), a high pass temporal filter, to zero the DC term and retrench the low-frequency terms, and then apply (2) for inverse Fourier transformation. Thus we got a sequence of images, in which the backgrounds (like ribs and tissues) were almost eliminated.

$$\overline{F}(x,y,k)=F(x,y,k)*H(x,y,k) \quad 0\le k\le T-1, \tag{3}$$

where $H(x,y,k)=\begin{cases}0 & \text{if } k=0\\ 1\text{ or}\le 1 & \text{if } k\neq 0\end{cases} \quad 0\le k\le T-1.$

We then use a matched filter to enhance arteries in the images obtained from the previous step. The details for computing the values in a matched filter may be found in [15]. In [15], the matched filter has orientation as its only parameter. Since we are interested in the coronary arteries that have different size, we expand the matched filter to have two parameters, i.e., the orientation and the size δ. The proposed matched filter has twelve orientations and six δ. There are 72 different filters to convolute the images. An angular resolution of 15° was used in the images. Since the vessel diameters of coronary arteries are different, we apply six δ for matched filters. For each orientation, the matched filters are obtained by using the transformation.

$$R_\theta\begin{bmatrix}\cos\theta & \sin\theta\\ -\sin\theta & \cos\theta\end{bmatrix}. \tag{4}$$

The size of a matched filter depends on δ, the larger δ the larger the dimension of filter. Fig. 1 shows a set of zero degree match filters with different δ.

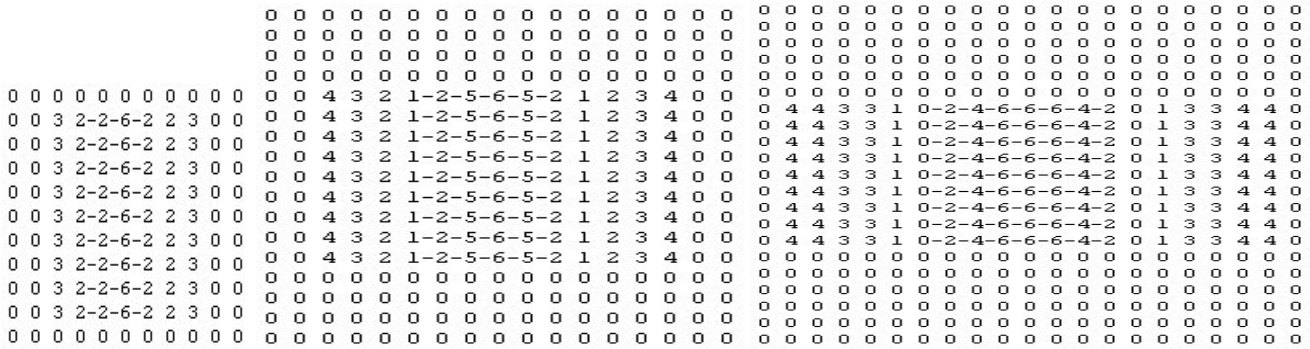

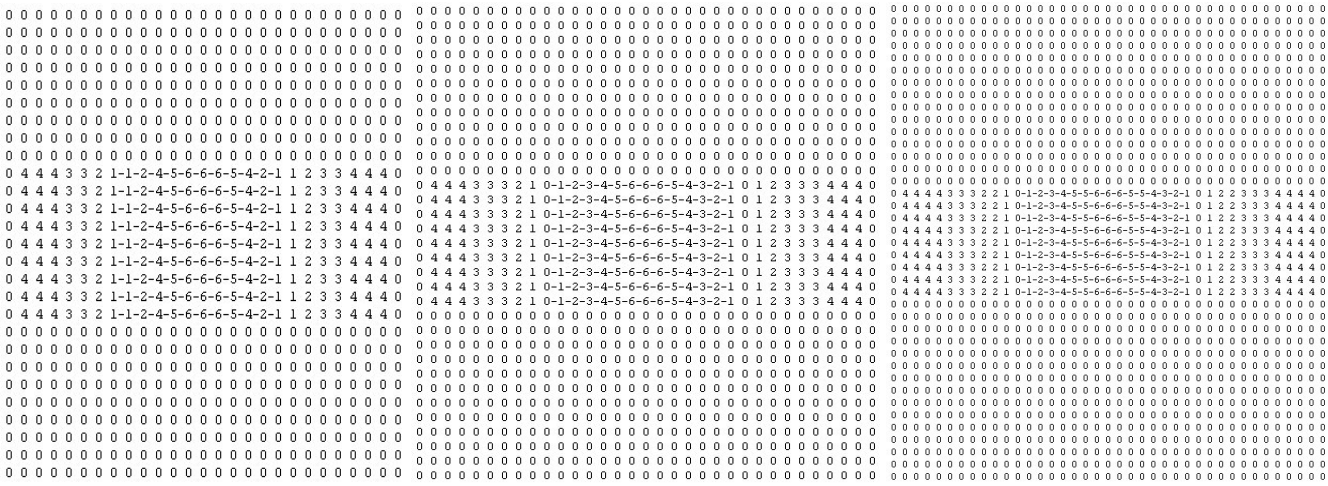

Fig. 1. Six matched filters that δ are 1, 2, …, and 6 with zero angle degree, respectively.

A set of 72 such filters are convolved to the angiographic images and only the maximum of their responses is retained. Since the filter will have its peak response only when it is aligned at an angle $\theta \pm 90°$. Thus, the filter needs to be rotated for all possible angles, and only leave the maximum response.

In designing a matched filter, we assume the backgrounds have constant intensity and are contaminated by white Gaussian noise. Real images, such as the angiographic images, contain low-spatial-frequency background, like ribs and other tissues, and high-spatial-frequency noise. These contaminations must be filtered to minimize loss of accuracy. Thus we need to apply previous Fourier preprocessing before match filter.

After processing of matched filter we get an enhanced image that usually contains some spike and spot. Now we apply the wavelet analysis to further remove the unwanted signal. Traditional pure-spatial analyses are a local transformation that difficult to analyze global information. While frequency analysis like Fourier transforms have a serious drawback in analysis of local information.. A filtering in frequency will cause lose the local property and cause probably severe ringing in spatial. We always lose accuracy in spatial when we gain accuracy in frequency. Thus, we need a compromise between spatial and frequency. Wavelet based transformation is useful for the sake of time-frequency description. The wavelet transformations are much more local than the pure Fourier transformations. The details for wavelet transformation can be found in [19]-[21]. In this work, we applied eight stages of discrete wavelet transformation Eq. (5) as show in Fig. 2. The first stage of wavelet transform split the image into four quarter-size images, upper left, upper right, lower left, and low right. The second stage also split the upper left image into four images. For subsequent stages, the upper left images are decomposed in exactly the same way to form four smaller images.

For a sequence of T images, denote as $f(x, y, t)$, the discrete wavelet transformation pair are

$$W(x, y, t) = DWT^8(f(x, y, t)) \text{ for } x,y \ \forall\, 0 \le t \le T-1, \tag{5}$$

$$f(x, y, t) = IDWT^8(W(x, y, t)) \text{ for } x,y \ \forall\, 0 \le t \le T-1, \tag{6}$$

where DWT^8 and $IDWT^8$ mean the eight stages of discrete wavelet transform and inverse transform, respectively.

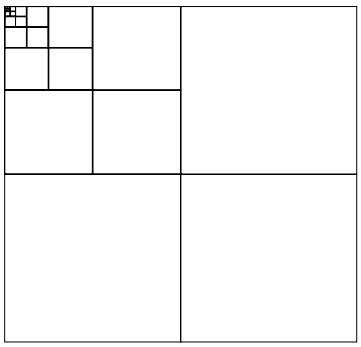

Fig. 2. The 2-D eight stages of discrete wavelet transformation.

Since wavelet transformations consider the spatial and frequency features. We apply Hamming window function [22]-[23] that was shown in Eq. (7) to the images in wavelet.

$$a_H(n) = \begin{cases} 0.54 + 0.4\cos\dfrac{2\pi n}{N-1} & \text{for } 0 \le n \le N\text{-}1, \\ 0 \end{cases} \tag{7}$$

where N is the number of stage of transformation in our case is eight.

And then we apply Eq. (6) in each stage for inverse transformation. We will obtain a better vessel image with lower noise. Thus we can preserve local features of the vessels and remove noise.

Since the vessels form a connected component in an angiographic image. The vessel in the stencil mask will form a very large connected component. Thus, we can remove smaller connected components that are formed by ribs, tissues, and noise. Especially, we find the ribs are difficult to remove from Eq. (3) exactly. Though they are removed mainly, this step can remove further. We define

$$scope(x,y) = \begin{cases} 0 & \text{if all } f(x,y,t) = 0 \\ 1 & \text{if there exist } f(x,y,t) \neq 0 \end{cases} \quad \text{for } t = 0,1,\ldots,T-1. \tag{8}$$

We apply a size filter for $scope(x,y)$, thus

$$stencil(x,y) = \begin{cases} 0 & \text{if the neighbors of } scope(x,y,t) < th \\ 1 & \text{otherwise} \end{cases} \quad \forall\ x, y. \tag{9}$$

$$\overline{f}(x,y,t) = \sum_{x=0}^{M-1}\sum_{y=0}^{N-1} f(x,y,t) * stencil(x,y) \quad \text{for } t = 0,1,\ldots,T-1. \tag{10}$$

We can find all connected components in the $\overline{f}(x,y,t)$. And then we apply the size filter to filter the small-connected components that are formed by noise and tissues. Finally, we use a histogram of previous processed images to threshold those images.

3. EXPERIMENTAL RESULTS

In this section, we present the results obtained by our methods. A sequence of X-Ray agiographic images that consist of 30 512x512 images is used in our experiment (Fig. 3). Fig. 4 shows one of angiographic images in the Fig. 3. Fig. 5 shows the

result of the matched filter that is consist of 72 different filters to convolute the images. The stencil mask is shown in Fig. 3 that consists of a number of only one connected component. Using the stencil mask we can remove background. Fig.7 shows the image in wavelet. We apply Hamming window function that was shown in Eq. (6) to the images in wavelet. Thus we can preserve local features, the vessels, and remove noise. Fig. 8(a) shows one of images that were processed using basic thresholding for comparison. Fig. 8(b) shows an examples result of our result obtained using our method. The results of a sequence of X-ray angiographic images are shown in Fig. 9. The proposed methods were implemented on a Pentium III PC under the Windows NT operating system. The overall execution time for a 512x512 image is usually less 10 minutes.

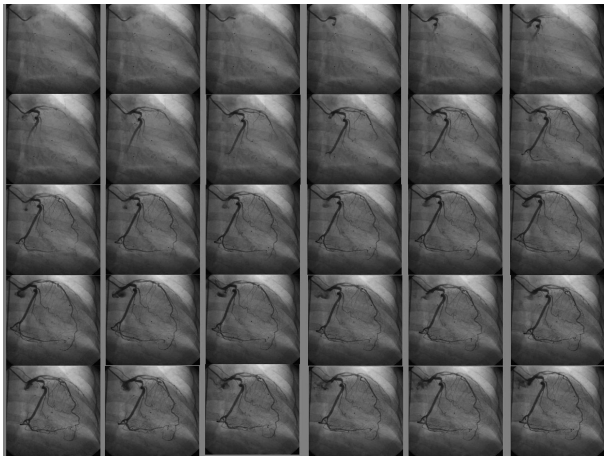

Fig. 3. A sequence of X-ray angiographic images used for our experiment.

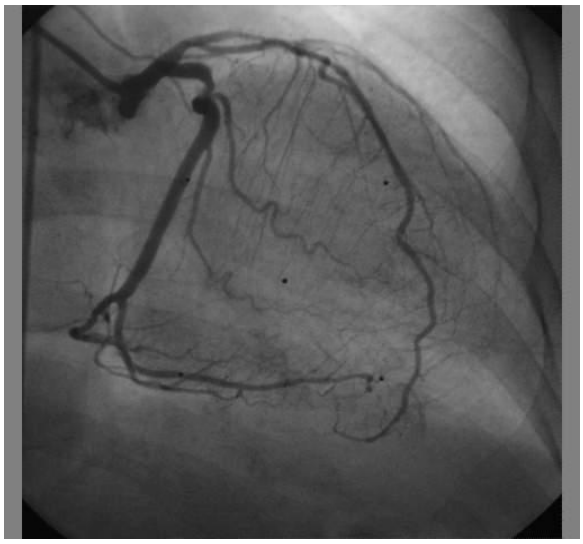

Fig. 4. An original angiographic image.

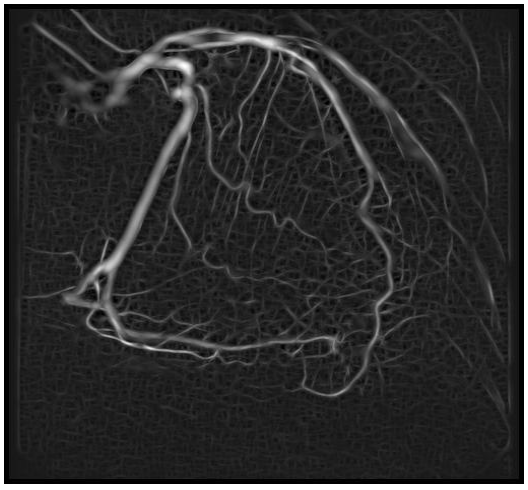

Fig.5. The result of the matched filter

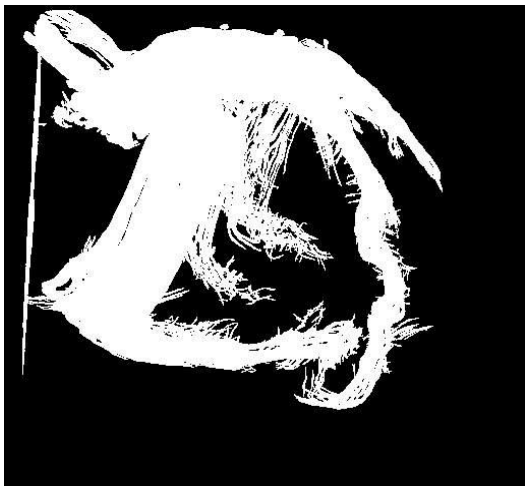

Fig.6. 2-D stencil mask that black denote 0 and white denote 1.

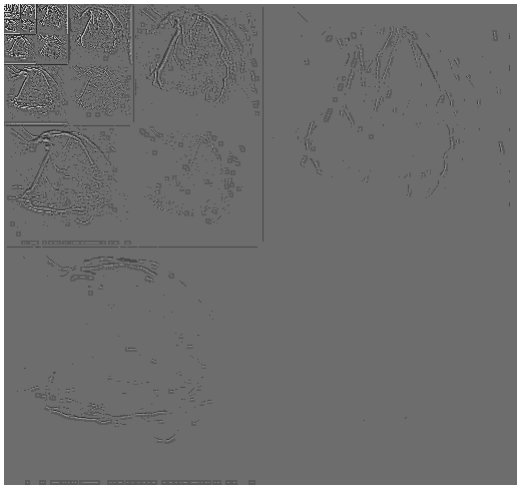

Fig. 7. The image in wavelet.

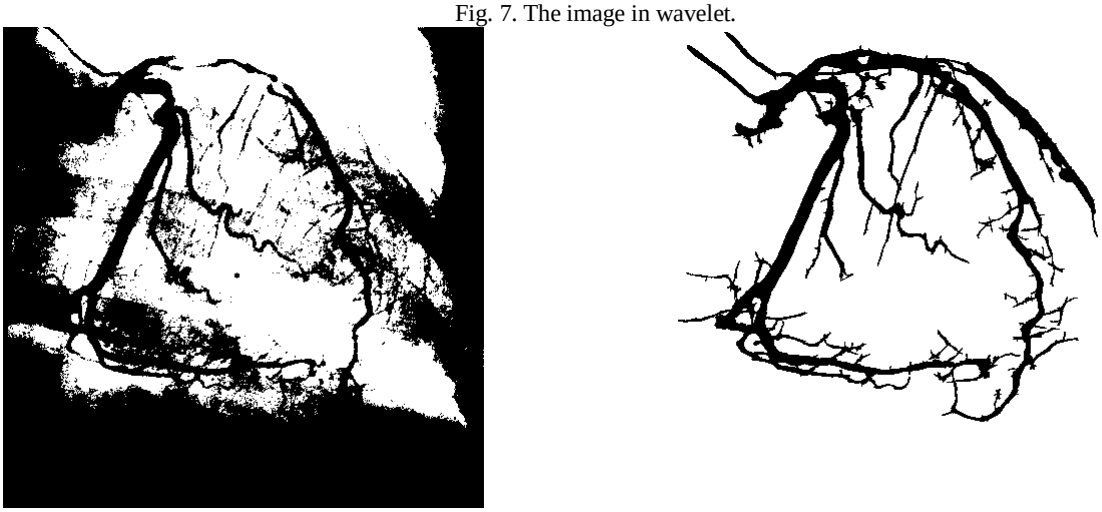

(b). (a)

Fig. 8. (a) The result of basic thresholding. (b) The result from our method

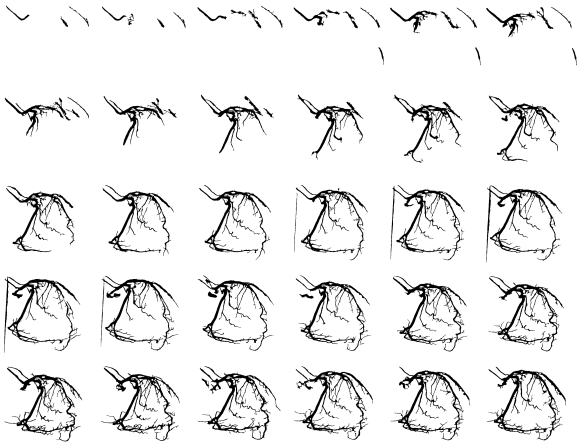

Fig. 9. The results of a sequence of X-ray angiographic images

REFERENCES

1. D. Marr and D. Hildereth, "Theory of edge detection," *Proc. Roy Soc, Ser. B,* vol. 207, pp. 187-217, 1980.
2. J. Canny, "A computational approach to edge detection," *IEEE Trans. PAMI,* vol. 8, pp. 679-697, Nov 1986.

3. T. Elfving, J. O. Eklundh and S. Nyberg, "Edge detection using the Marr-Hildreth operator with different sizes," in *Int. Conf. On Pattern Recognition*, pp. 1109-1112, 1982.
4. W. Frei and C. C. Chen, "Fast boundary detection: A generalization and a new algorithm," *IEEE Trans. Comput.*, vol. 8, pp. Oct. 1977.
5. F. M. Dickey, K. S. Shanmuugam, and J. A. Green, "An optimal frequency domin flter for edge detctionin digtal pictures," *IEEE Trans. Anal, Machine Intell.*, vol. PAMI-1, pp. 37-49, Jan. 1979.
6. J. W. Modestino, and R. W. Fries, "Edge detection in noisy images using recursive diital fitering," Comput. *Graphics Image Processing*, vol. 6, pp. 409-433, 1977.
7. V. Torre and T. A. Poggio, "On edge dection, *IEEE PAMI.*, vol. PAMI-8, pp. 147-163, Mar. 1979.
8. P. H. Eichel, E.J. Delp, K. Koral, and A. J. Buda, "A method for fully automatic definition of coronary arterial edges from cineagiograms," *IEEE Trans. Med. Imaging*, vol. 18, pp. 313-320, 1988.
9. K. Haris, S. N. Efstratiatiadis, N. Magkaveras, C. Pappas, J Gourassas, and G. Louridas, "Model based morphological Segmentation and labeling of coronary artery angiograms," *IEEE Trans. Med. Imaging*, vol. 18, pp. 1003-1015, 1999.
10. N. Ezquerra, S Capell, L. Klein, and P. Duijves, "Model-Guided Labeling of Coronary Structure," *IEEE Trans. Med. Imaging*, vol. 17, no. 3, jun. pp 429-441, 1998.
11. R. C. Chan, W. C. Karl, and R. S. Lees, "A New Model-Based Technique for Enhanced Small-Vessel Measurements in X-Ray Cine-Angiograms," *IEEE Trans. Med. Imaging*, vol. 19, pp. 243-255, Mar., 2000.
12. Y. Sun, "Automated identification of vessel contours in coronary arteriograms by an adaptive tracking algorithm," *IEEE Trans. Med. Imaging*, vol. 8, pp. 78-88, Mar., 1989.
13. S. Tamura, K. Tanaka, S. Ohmori, K. Okazaki, A. Okada, and M. Hoshi, "Semiautomatic leakage analyzing system for time series fluorescein ocular fundus angiography," *Pattern Reconition*, vol. 16, no. 2, pp. 149-162, 1983.
14. Y. Tolias and S. Panas, "A fuzzy vessel tracking algorithm for retinal images based on fuzzy clustering," *IEEE Trans. Med. Imaging*, vol. 17, pp. 263-273, Apr., 1998.
15. S. Chaudhuri, S. Chatterjee, N. Katz, M. Nelson, and M. GOLDBAUM, "Detection of blood vessels in retinal images using two-dimensional matched filter," *IEEE Trans. Med. Imaging*, vol. 8, pp. 263-269, 1989.
16. A. Hoover, V. Kouznetsova, and M. Goldbaum, "Locating Blood Vessels in Retinal Images by Piecewise threshold probing of a matched filter response," *IEEE Trans. Med. Imaging*, vol. 8, pp. 203-210, 2000.
17. Y. Sun, R. J. Lucariello, and S. A. Chiaramida, "Directional Low-Pass Filtering for Improved Accuracy and Reproducibility of Stenosis Quantification in Coronary Arteriograms," *IEEE Trans. Med. Imaging*, vol. 14, No2., pp. 242-248, Jun.,2000.
18. R. C. Gonzalez, and R. E. Woods, "Digital Image Processing," *Addison-Wesley Publishing Company*, pp 81-125, 1992.
19. S. Mallat, "A Theory fro Multiresolution Signal Decomposition: The Wavelet Representation," *IEEE Trans.PAMI*, vol. 11, pp. 647-693, 1999.
20. P. P. Vaidyanathan, "Multirate Systems And Filter Banks", *Prentice Hall, Inc.*, 1993.
21. L. Cohen, "Time-Frequency Distributions - A Review," *Proc. IEEE, Vol. 77*, pp. 941-981, 1989.
22. L. Rabiner, and B. Gold, "Theory and Application of Digital Signal Processing," *Prentice Hall, Inc.*, 1975.
23. D. J. DeFatta, J. G Luucas, and W. S.odgis, "Digital Signal Processing," *Prentice Hall, Inc.*, 1975.